Abdelfatah N. Aborobaa
Master student.
Military technical college, Cairo
Egypt

Khaled A. Ghamry
Doctor
Military technical college, Cairo
Egypt

Amr Saleh
Doctor
Military technical college, Cairo
Egypt

Mohamed H. Mabrouk
Professor
Military technical college, Cairo
Egypt

Sensorless Position Estimating and Transition time Identifying for the spool of a High Speed on/off Solenoid Valve

In this paper, a sensorless method of detecting the spool position of a high-speed on/off solenoid valve is presented. The method depends on analyzing the time-current curve of the solenoid coil passing current and measuring the maximum stroke of the valve spool, such that the dynamic behavior of the valve is estimated and the spool displacement curve is plotted. A mathematical model of the solenoid valve is developed and the effect of the hydraulic force on the valve spool is studied. Experimental results show that the proposed method error is less than 7% when compared to valve spool displacement measured by the commonly used linear variable displacement transducer.

Keywords: *high speed on/off valves, solenoid valve, displacement sensors.*

1. INTRODUCTION

Recently solenoid control methods have received growing attention. A solenoid refers to a device that converts energy to motion. It consists of a coil wound into a tightly packed helix usually its length is greater than its diameter and is often wrapped around a metallic core. Therefore, when the current passes through its coil, a uniform magnetic field is produced [1].

The solenoid is an essential component for high-speed on/off valves (HSV) which are commonly used in hydraulic and pneumatic systems such as aircraft [2], automobiles [3], construction equipment [4], and others.

Although conventional proportional/servo valves have been employed in many applications due to their high-frequency response [5], they have the disadvantages of high cost, high power consumption, high sensitivity to contamination, and as a result low reliability [6].

On the contrary, HSV is considered as a competitive alternate to proportional/servo valves due to their low cost, high efficiency as well as high reliability [7]. Moreover, HSV can be actuated either by a solenoid, magnetostrictive [8], or piezoelectric actuators [9]. Alt–hough the solenoid actuator has the advantages of lower cost, smaller size and larger displacement with 12 or 24 volt DC rated voltage. When the solenoid is energized, the spool does not move instantaneously and takes time to reach its maximum stroke [10]. Similarly, when the solenoid is de-energized, the spool does not return to its neutral position instantaneously. These delays usually are not specified in the valve datasheet. Therefore, experimental measurements are needed to identify the position-time curve of the valve spool [11].

Many studies have been carried out to improve the performance of the solenoid valve and convert it to a proportional device by applying various control techniques [12]. Kang and Jeon used a fraction PD controller to control the position of the solenoid valve [13]. While Malaguti and Pregnolato applied a nonlinear robust control technique to produce a proportional action from an on/off solenoid [14]. Lunge et al. used sliding mode control to ensure the desired position of the solenoid plunger [15]. Such studies and others require accurate knowledge of spool displacement response [16].

Measuring the spool displacement can be performed directly by using a displacement transducer or indirectly by measuring a relevant property such as pressure to indicate the spool movement. For example, Hammond used a Hall sensor for position sensing in [17]. However, the Hall sensor may be not able to detect slow movement of the plunger. A laser sensor is used to measure the spool displacement by Lee et al. [18]. Scheidl et al. used an eddy current for spool position measuring [19]. However, using such methods require access to the valve itself which is sealed to provide pressure balancing and debar leakage or mucking. For these reasons, valve accessing will affect its properties.

Zhong et al. used a pressure sensor to indicate the spool movement [20]. Generally, the pressure drop across the valve is affected by many factors such as valve orifice area (which indicates the spool position), valve flow rate, oil density (which changes with operating temperature). Due to these factors, using a pressure sensor to indicate the valve spool displacement may have some accuracy problems.

The additional cost and space taken by the sensor are considered. So a sensorless method may be desired. Braun et al. utilized a technique of observing the back electromagnetic force (EMF) induced in the solenoid during the plunger movement [21]. A precise estimation of the actuator position is achieved at high speed. On the other hand, the back EMF is disappeared at low speed, so, the technique is not able to operate.

Yudell and Van de Ven proposed a method to identify the beginning and end of valve transition times without modification of the valve body [22]. This

Received: September 2021, Accepted: October 2021
Correspondence to: Abdelfatah N. Aborobaa
Military technical college, Ismail Al Fangari, El-Qobba Bridge, Cairo, Egypt.
E-mail: abdelfatah.nader@mtc.edu.eg
doi: 10.5937/fme2201099A

method depends on measuring the passing current through the solenoid while it is fully open as well as fully closed hence analyzing the two current curves. Therefore, many highly precision – were done to identify the transition times. However, the valve spool displacement curve could not be obtained.

In this paper, the proposed method aims to identify the valve spool displacement curve without any modification of the valve body. The method depends on measuring the solenoid passing current and its maximum stroke. An explanation of valve construction and its principle of operation are presented in section 2. A mathematical model of the solenoid operation and factors affecting the passing current is presented in section 3. The experimental work is explained in section 4 while the results are discussed in section 5 and finally followed by conclusions in section 6.

2. SOLENOID CONSTRUCTION

A solenoid is an electromagnetic actuator used for either linear or rotary actuation for valves. It is made of a coil wound on a nonmagnetic metal called a bobbin to prevent a flux short circuit between the coil and plunger. A fixed frame which is a high permeability material used to guide the magnetic flux, in addition to a movable plunger and a stop is shown in figure 1 [23].

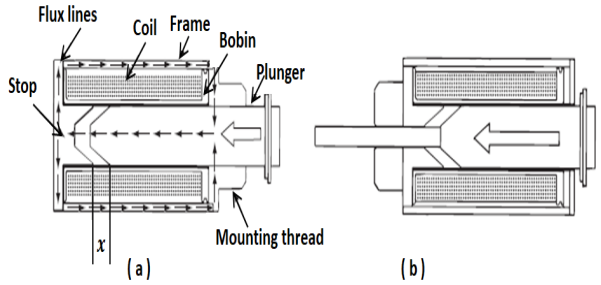

Figure 1 Solenoid construction and its components. (a) pull-type and (b) push type [23].

When the solenoid is energized, an induced magnetic field is generated inside the coil. The ferromagnetic plunger tends to increase the flux linkage by moving towards the stopper to close the air gap. Therefore, the plunger always works on the pull principle, but pull or push motion can be obtained by mechanical design, as shown in Figures 1 (a) and (b).

The generated magnetic force is proportional to the number of coil turns, squared of the passing current, and inversely proportional to the square of the air gap [23]. Regarding decreasing the air gap, the reluctance of the magnetic flux path decreases. Consequently, the generated magnetic force is increased.

Figure 2 shows the relation between the generated magnetic force and the plunger displacement under a constant current. Also, it shows that the curve relating to force and displacement is influenced by the plunger and the stop shape. For small solenoid strokes (< 1.5 mm), it is recommended to use a flat shape plunger as the generated force is about three to five times greater than a 60° conical face plunger. However, for larger strokes (< 19 mm), a conical face plunger is recommended as it offers a larger force. In addition to several coil turns, electric current, air gap, the magnetic force is also a function of the solenoid shape design, the material permeability, and temperature [24].

For a solenoid, its design and coil turns are constant while air gap and material permeability vary with the plunger displacement. Temperature mainly affects the coil resistance which leads to a change in the coil current for a given voltage. If the control system prevents the variation of the coil current, the temperature effect can be neglected [24]. For a specific solenoid, the generated magnetic force is a function of the plunger displacement and passing current.

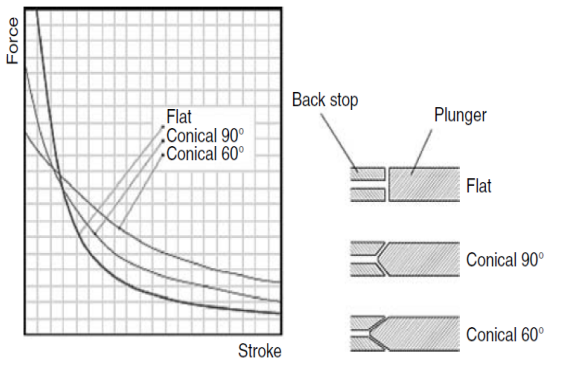

Figure 2 The generated magnetic force versus the plunger displacement for different plunger and stop designs [24].

3. MATHEMATICAL MODEL

The solenoid valve system can be divided into two main subsystems, electro-magnetic subsystem, and mechanical subsystem, as shown in figure 3.

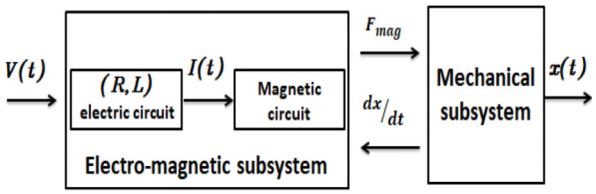

Figure 3 Mathematical model representation.

3.1 Electro-magnetic subsystem

The model for this subsystem has to transform the applied input voltage to the produced magnetic force, which in turn, represents the valve driving force. Moreover, the magnetic force is generated from the interaction between the electromagnetic field and the variable reluctance of the air gap. Leakage and fringing flux is neglected and the flux density is considered constant through the plunger and the stop [25].

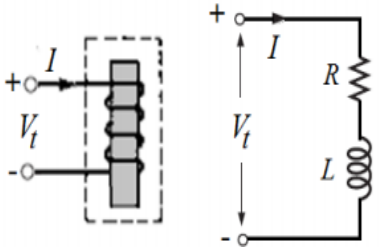

Figure 4 Representation of the electro-magnetic subsystem of solenoid model [25].

The circuit shown in figure 4 represents the electromagnetic subsystem of the solenoid. It considers the solenoid as an inductor connected in series with a resistor. So, by applying Kirchhoff's voltage law, the total voltage can be expressed as:

$$V_t = V_R + V_L \tag{1}$$

$$V_t = iR + i\frac{dL}{dt} + L\frac{di}{dt} \tag{2}$$

where:
V_t … the solenoid coil applied voltage (volt).
V_R … the solenoid coil resistance voltage (volt).
V_L … the solenoid coil inductance voltage (volt).
i … the coil passing current (amp).
R … the coil resistance (ohm).
L … the coil inductance (H).

The coil inductance L can be expressed as:

$$L = \frac{N^2}{\Re_{tot}} \tag{3}$$

where, N is the number of solenoid coil turns and $\Re_{tot}$ is the total reluctance of the magnetic circuit in the air gap, fixed members, and movable plunger, which is inversely proportional to the material permeability [26].

Since the frame, the stop, and the plunger has high permeability compared to air, then the magnetic reluctance in fixed and movable materials can be neglected and only the air gap reluctance is considered. Therefore, Equation (3) becomes:

$$L = \frac{N^2}{\Re_{gap}} \tag{4}$$

$$\Re_{gap} = \frac{g_t - x}{\mu_0 A} \tag{5}$$

where: $\Re_{gap}$ … the reluctance of the air gap (H^{-1}).
x … valve spool displacement (m).
g_t …. the total length of the air gap (m).
μ_0 … the permeability of air (H/m).
A … the air gap cross-section area (m^2).

When the solenoid is energized, the plunger moves to close the air gap. Therefore, x equals x_{max} at the end of the spool stroke where the air gap is eliminated and becomes a magnetic short circuit.

From equations (4) and (5):

$$L = \frac{N^2 \mu_0 A}{(g_t - x)} \tag{6}$$

Equation (6) shows that the coil inductance is a function of the displacement x when other affecting parameters are considered constant for a certain valve [27]. The spool or plunger displacement is time-dependent; consequently, the coil inductance is time-dependent as well. Its time derivative can be expressed as

$$\frac{dL}{dt} = N^2 \mu_0 A \frac{1}{(g_t - x)^2}\frac{dx}{dt} \tag{7}$$

From equations (6) and (7),

$$\frac{dL}{dt} = \frac{L}{(g_t - x)}\frac{dx}{dt} \tag{8}$$

Substituting in (2),

$$V_t = iR - i\frac{L}{(g_t - x)}\frac{dx}{dt} + L\frac{di}{dt} \tag{9}$$

The current derivative,

$$\frac{di}{dt} = \frac{1}{L}(V_t - iR) + \frac{i}{(g_t - x)}\frac{dx}{dt} \tag{10}$$

3.2 Mechanical subsystem

The magnetic force is the motivating force that causes the valve spool to move. Therefore, it has to overcome the resistance forces such as friction force, damping force, and hydraulic force. It is a function of the coil current and plunger displacement, and can be expressed as [28]:

$$F_{mag}(i,x) = \frac{1}{2}\mu_0 N^2 A\left(\frac{i}{(g_t - x)}\right)^2 \tag{11}$$

The mechanical subsystem model can be presented as:

$$m\ddot{x} = F_{mag} - k_s x - c\dot{x} - f_{hyd} \tag{12}$$

where:
m …. the mass of the moving parts (kg).
k_s …. the spring stiffness (N/m).
c …. the damping coefficient (N.s/m).
f_{hyd} … the flow force (N).

Figure 5 shows the effect of hydraulic flow force on the valve spool, where v_1 is the velocity in the valve chamber, while v_2 is the outlet velocity in the throttle section.

F_r is the radial component of the jet force, if the inlet and outlet ports are distributed symmetrically, the components of the force will compensate each other, otherwise, these forces may increase the wear and friction of the spool.

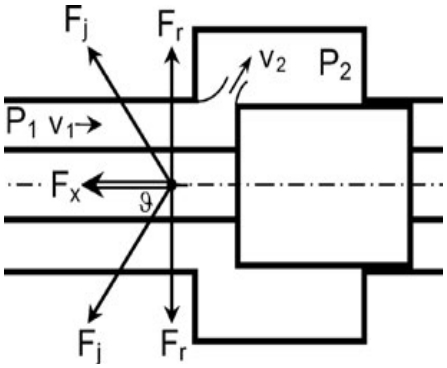

Figure 5 The effect of hydraulic flow force on the valve spool.

The jet force axial component F_x is added to each other and acts in the direction to close the valve. This force is deduced in [29] and is shown to be a function of the spool displacement as follows:

$$f_{hyd} = f_x = 0.428\omega\Delta \mathrm{Px} \tag{13}$$

where ω is the valve throttling area proportionality coefficient and ΔP is the pressure difference between spool inlet and outlet sides.

The electro-magnetic subsystem in equation (10) shows that the factors affecting the current derivative and hence the time-current curve presented as the source voltage, the coil electric resistance, the coil inductance, the current, and plunger or spool valve displacement as well as its velocity.

As the source voltage is DC, the electric resistance of the coil is assumed to be constant. The coil inductance is a function of valve spool displacement x. Therefore, the slope of the current curve depends mainly on spool displacement. Accordingly, the proposed method uses this fact to estimate the spool displacement start and endpoints.

The mechanical subsystem model represented by equations (11-13), shows that the dynamics of the valve spool depend on the coil electric current, the spool position, and its derivatives. It means that the magnetic force (the coil current) varies according to the valve spool motion restriction forces. Consequently, the displacement curve of the spool will change according to the current change.

The mechanical sub-model declares the effect of the hydraulic force on the valve spool dynamic. Equation (13) shows that the hydraulic force is the function of the valve position as well as the pressure difference between both sides of the valve spool.

4. EXPERIMENTAL SETUP

In this research, hSV-6432-C 4/3 solenoid operated directional control valve is used. Figure 6 shows that the used valve is a double-acting one, with two solenoids for spool movement control and two holding spring for the neutral position

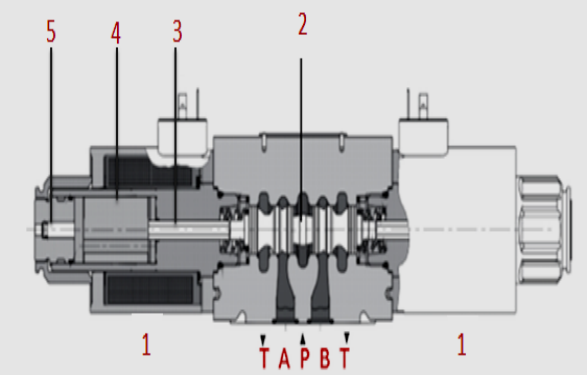

Figure 6 Cross-section of 4/3 solenoid operated direction control valve; (1) solenoids on each side, (2) spool, (3) plunger, (4) core tube, (5) press pin, and ports (T, A, P, and B).

The mathematical model shows that the solenoid time-current curve slope is being changed with the valve displacement. Therefore, for validation, the valve spool is fixed stationery at two different cases, neutral position, and maximum stroke position. In these two cases, the solenoid is subjected to an excitation pulse input voltage and the solenoid coil electric current is measured. A jaw is used to ensure the fixation of the solenoid plunger at these two positions.

The valve model also shows that the hydraulic force is a valve spool centering force and it is increasing proportionally with increasing the pressure difference at both sides of the valve spool. Consequently, incrassating the pressure difference will increase the hydraulic force. Since the valve spool movement restriction force is increased, the magnetic emotional force should be increased to overcome these rest–reactions. Therefore, more electric current is required.

To validate that, the hydraulic circuit shown in figure 7 is installed to measure the effect of hydraulic force on the dissipated current, consequently its effect on the magnetic force and valve dynamics.

In the hydraulic circuit shown in figure 7, the relief valve (2) is used to control the solenoid valve (4) supply pressure which is indicated by the pressure gage (3), as the valve return port is connected to the tank, so the pressure difference is equal to the gauge pressure.

The adjusting screw in the relief valve is rotated until a certain pressure value is reached, at that value the solenoid passing current is measured when the valve is energized and de-energized. Further current measurements are performed at different values of supply pressure as well as when no oil flows through the valve.

The proposed method of estimating the spool displacement is verified by measuring the spool displacement via WA/10mm inductive displacement transducer of WA-L series. This series is characterized by a loose plunger feather and a compact dimension design related to the measuring range [30]. This compact design is due to the that the sensor has an active quarter bridge circuit based on the principle of the differential inductor.

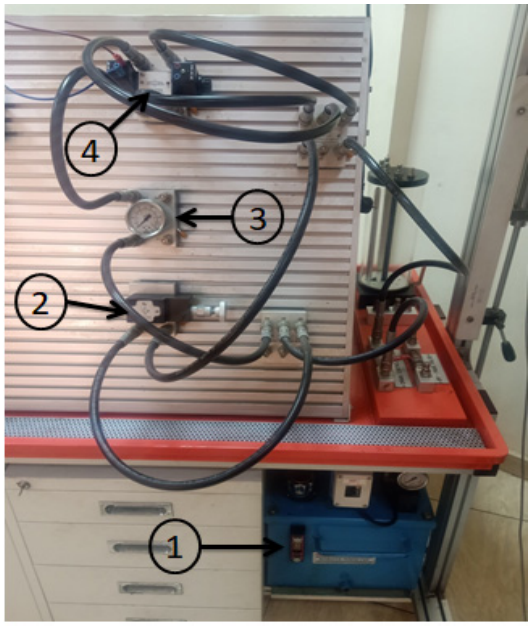

Figure 7 hydraulic circuit used to measure the effect of hydraulic force on solenoid valve spool dynamics. (1) hydraulic tank, (2) pressure relief valve, (3) pressure gauge, (4) solenoid valve.

This circuit and the sensor form together with a full-bridge circuit that makes the connection of the WA-L transducer to the measuring amplifier easy. In

addition, the series has a rugged mechanical construction, a stable temperature behavior, and is non-sensitive to dirt.

To connect the sensor to the spool, one of the two sides solenoids is replaced with a typical fabricated holed nut. A small threaded rod is welded to the spool passing through the nut hole and connected to the sensor through one nut. These modifications of the valve are shown in figure 8.

From equation (13), the flow force is very small compared to the other forces, and it is a function of the spool displacement. Moreover, the experimental work is carried out without flow after installing LVDT to prevent leakage.

Figure 8 Modifications applied to the solenoid valve to be able to connect the LVDT.

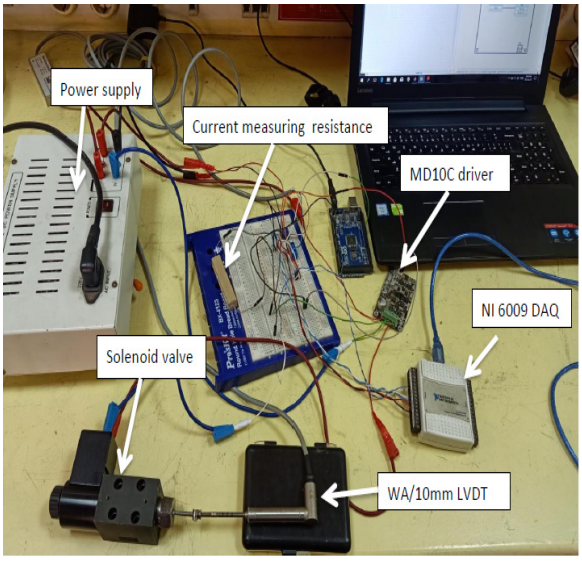

Figure 9 Experimental setup includes LVDT, power supply, driving card, and the current measuring resistance.

A 24 volt DC power supply is used to feed both the valve solenoid and the displacement sensor. As the rating voltage of the solenoid is 24 volt and the power input to the sensor ranges from 15 to 30 volt, so only one power supply can be used. The displacement sensor LVDT output voltage ranges from 0.5 to 10 volts according to the position of the plunger

A NI 6009 data acquisition card (DAQ) is used to read data since the maximum input voltage to the DAQ is 10 volt (according to card specification -10 to 10 volts). To prevent DAQ damage, two equal resistances are used to divide the output voltage of the displacement sensor. In addition, a 1 ohm 10%20W resistor is connected in series with the solenoid coil to measure the passing current.

This resistor is made of ceramic and its rated power is 20 watt to withstand the voltage applied and high current consumed. Additionally, DAQ is used to measure the voltage drop value over that resistance which equals 1 ohm. So, it is equal to the value of its flowing current. Consequently, the solenoid current is deduced.

To control the input signal from the power supply, a MD10C driver is used it can sustain up to 30volt DC voltage, and up to 13amp DC or 30amp peak (10 sec). It is a fast response time solid-state component that can eliminate the wear and tear of mechanical relay. The MD10C driver's control input signal is from 3.3 volt to 5 volt, so it is compatible with Arduino and Raspberry Pi. An Arduino mega 2560 is used to send the control input signal, as shown in figure 7.

Arduino Mega 2560 is used to generate a repeated pulse input signal of frequency equals 0.5 Hz and amplitude equals 5 volt, to the driver card to energize the solenoid on and off repeatedly.

In addition, a TDS5054B digital phosphor oscilloscope is used to compare the control input signal to the solenoid coil input voltage. Two channels of the oscilloscope are used; one channel is used to measure the input control signal while the other is used to measure the solenoid voltage.

Figure 10 shows an input voltage that equals 5 volts, which acts as the control input signal to the driver card to produce a 24 volts output voltage to the solenoid.

The control input signal is produced from Arduino and its rated voltage is about 5 volt which can be easily measured by data acquisition card, while it is difficult to measure the solenoid voltage with that card.

The proposed methodology depends on two main steps, 1. Measurement of the maximum stroke of the valve spool, 2. Analysis of the time-current curve.

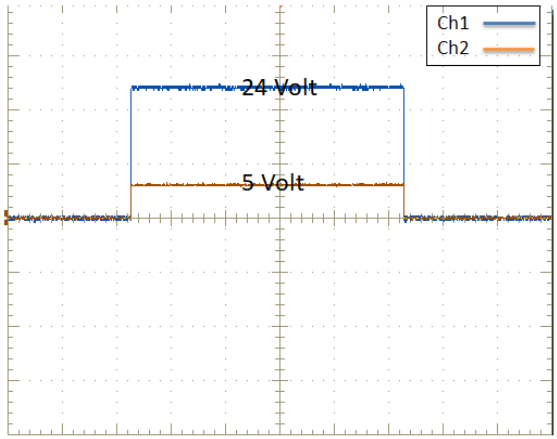

Figure 10 The relation between the input control signal voltage and the excitation solenoid coil voltage.

Measuring the valve spool maximum stroke is carried out as follows: at the valve neutral position, an Allen key is used to push the press pin until ensuring that the core tube is in contact but not pushing plunger (3) as shown in figure 6. On that position, and by using a vernier caliper, the distance between the press pin and coil stage is measured, the solenoid is energized, and again by the Allen key, the pin is ensured to touch not push the plunger. The same distance is measured again.

Finally, this process is repeated and the difference between the two measured distances is measured for every trial, which indicates the valve spool maximum stroke. These trials are done to make sure that the result is accurate which shows that the valve spool stroke is 1.76 mm.

5. RESULTS AND DISCUSSION

Experimental current measurements when the solenoid is energized and de-energized while its plunger is kept fixed at two different positions, initial and maximum stroke positions are shown in figure 11.

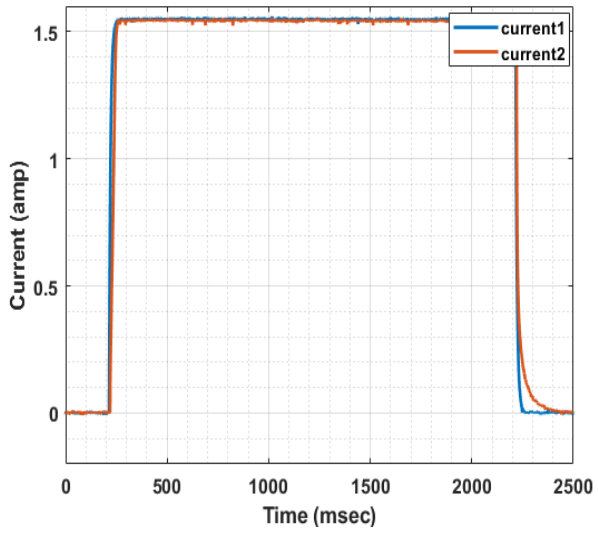

Figure 11 Measured current when the solenoid plunger is fixed. Current1 when $x=0$, current2 when $x=x_{max}$

The results show that the current increases exponentially from zero to its maximum value when the solenoid is energized, the slope of the curve does not change until the current reaches that value. The same behavior happens when the solenoid is de-energized, current drops to zero exponentially with no observed change in the curve slope.

The results also show that the slope of the curve when the plunger is fixed at its initial position differs from that when the plunger is fixed at its maximum stroke. That is because the inductance of the solenoid is different at the two positions.

The result of current measured under different valve spool pressure differences and when no hydraulic force is applied on the valve spool when the solenoid is energized and when it is de-energized are shown in figures (12 and 13) respectively.

Figures 12 and 13 show that solenoid dissipated current is increased as the pressure difference is increased. Peaks and troughs of the current curve, which indicate the valve spool dynamics, have different values and occur at various times. Those changes are shown clearly when the valve is energized. So the dynamics of the valve spool are affected by the hydraulic force.

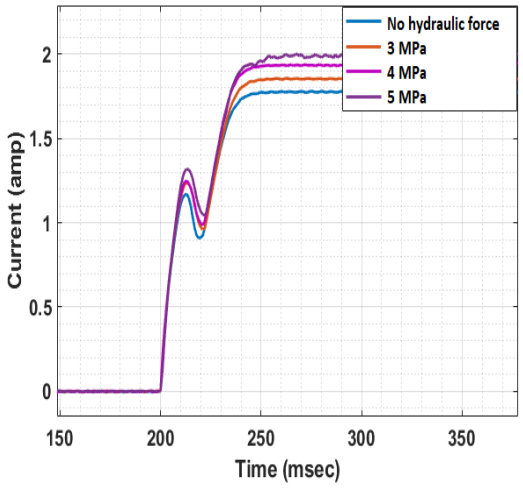

Figure 12 Current measured when the solenoid is energized under no applied hydraulic force and pressure difference ΔP = 3MPa, 4 MPa, and 5 MPa.

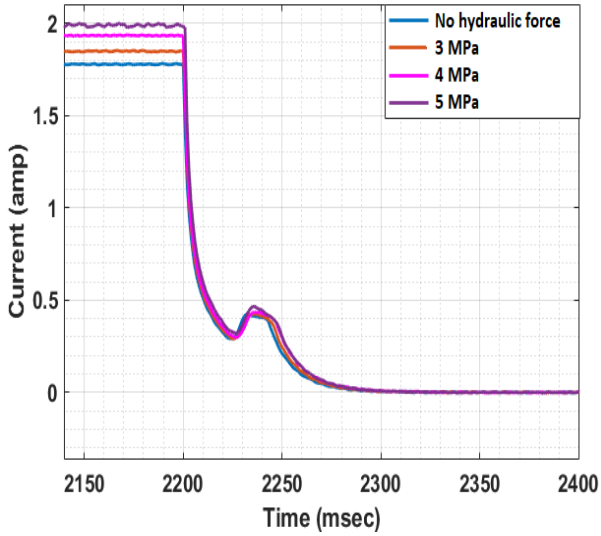

Figure 13 Current measured when the solenoid is de-energized under no applied hydraulic force and pressure difference ΔP = 3MPa, 4 MPa, and 5 MPa.

When the solenoid is de-energized, the valve spool dynamics seems to be the same under different conditions, that is because, for the used valve, when the solenoid is de-energized the valve return to its neutral position at which no oil flows through the valve as explained at the previous section, so there is no change in valve spool dynamics.

That means for another solenoid valve for which either when its solenoid is energized or de-energized hydraulic oil flows through its spool and the dynamics of the valve spool will change at the two conditions when the hydraulic force is changed.

The solenoid coil passing current and spool displacement due to solenoid valve excitation voltage are measured and plotted as shown in figure 14.

The figure shows that the coil current does not reach its maximum value immediately when the solenoid is energized. Additionally, the slope of the

current curve changes twice after the coil is energized and before the current reaches its maximum value. In the case of de-energizing of the coil, the current does not collapse immediately while its curve slope changes twice after de-energizing and before reaching its minimum value.

The figure also shows the relation between the displacement and the current one in which the proposed methodology is designed.

Whenever a current is passing through the wire wound into the solenoid coil, a concentrated magnetic field is stored in it. Once the solenoid is excited, the current increases, triggering the magnetic field to expand until being enough to overcome the armature moving resistance forces.

When the armature moves, it causes an increase in the magnetic field concentration. This is because the armature's magnetic mass is moving further into the magnetic field. Because the change in the magnetic field is in the same direction as the current creating it, an opposing voltage is induced into the winding. As a result, the field causes a reduction in the current while the armature moves.

After the armature reaches its maximum stroke, the current increases again on its upward path until it reaches its maximum value. Similarly, this is what happens when the solenoid is de-energized.

Figure 15 shows the current analysis curve when the solenoid is energized and the corresponding predicted displacement which can be explained as follows:

At point 0 (time = 0.1 sec), the solenoid is energized and the current starts to increase. At point 1 (time = 0.114 sec), the magnetic field is now able to move the armature. Therefore, there is no movement in the valve spool from point 0 to point 1.

After the current reaches point 1, it drops down due to the movement of the solenoid armature until reaching point 2 (at time = 0.119 s). So, the valve spool starts moving from point 1 reaching its maximum value (1.76 mm as measured) at point 2.

The current continues to increase until reaches its maximum value at point 3.

When the solenoid is de-energized, the current curve and the corresponding indicated displacement are plotted in figure 16 and are analyzed as follows:

From point 3 to point 4, both the current and displacement are at their maximum values.

When the solenoid is de-energized at point 4 (at time =2.101 sec), the current starts to drop up to point 5 (at time =2.141 sec), where an increase in current occurs due to the movement of the armature. So, from point 4 to point 5 there is no movement in the valve spool and the spool starts moving back to its initial position at point 5. The current returns to drop again at point 6 (time = 2.147 sec), where the armature stops moving and the spool returns to its initial position.

The results of the proposed method are compared with the results of the LVDT when the solenoid is energized and de-energized, as shown in figures 17 and 18 respectively.

The root means square error (RMSE) is calculated for the measured data using LVDT and the data estimated from the proposed method. Equation (14) is commonly used to express the value of RMSE [31].

$$RMSE = \sqrt{\frac{1}{N}\sum_{i=1}^{N}(D_{meas} - D_{est})^2} \tag{14}$$

where N … The number of samples used.
D_{meas} …. The measured spool displacement.
D_{est} … The estimated spool displacement.

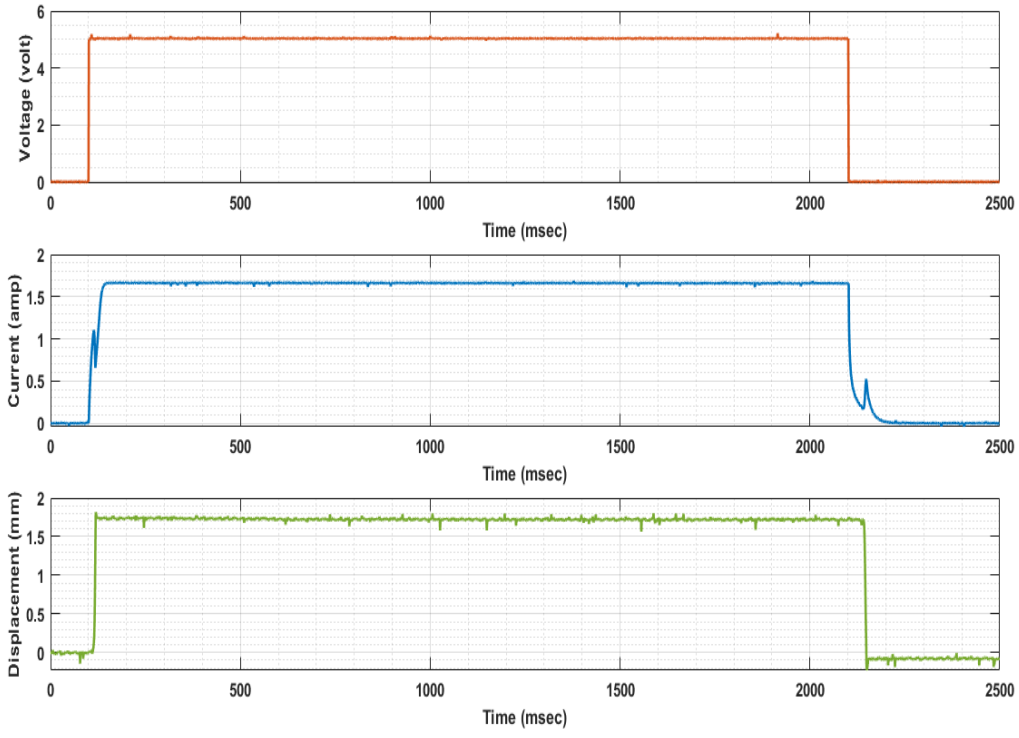

Figure 14 The solenoid exciting voltage and the corresponding solenoid coil current and valve spool displacement. The valve supply pressure equals 3 Mpa.

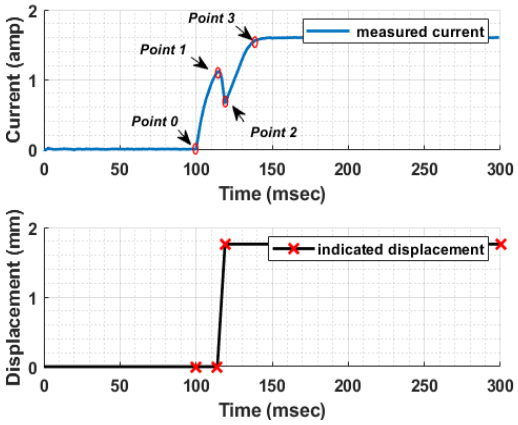

Figure 15 Current analysis when the solenoid is energized and the corresponding indicated displacement.

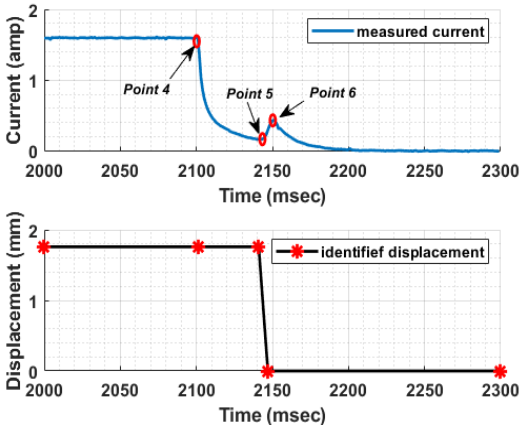

Figure 16 Current analysis when the solenoid is de-energized and the corresponding indicated displacement.

Linear interpolation is done between every two successive identifying points at the estimation data to adequate the number of samples in both measuring and estimation data. RMSE is measured for the data shown in both figures 17 & 18 and it is about 7 %. This value can be reduced by modifying the LVDT fixation, valve fixation, and filtering the measured data by removing the noise.

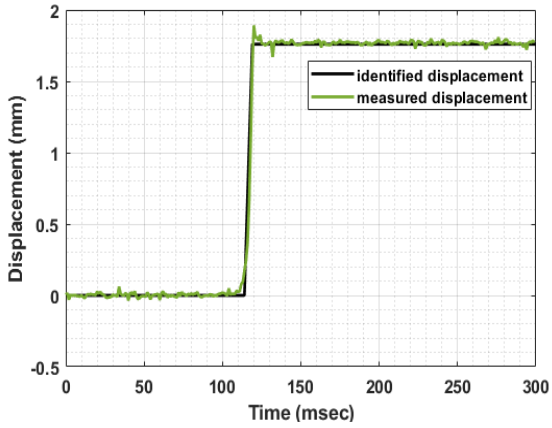

Figure 17 Comparison between identified and measured displacement when the solenoid is energized

The proposed method is implemented using Matlab software code. This code is valid for different operating conditions of any solenoid valve to identify the valve spool displacement using the solenoid current.

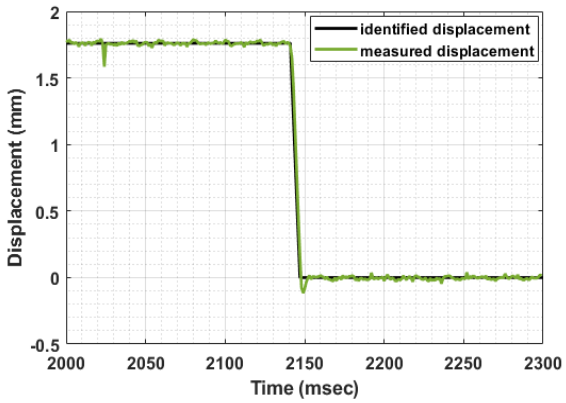

Figure 18 Comparison between identified and measured displacement when the solenoid is de-energized.

In addition to the current data, the maximum stroke of the valve spool should be input into the code. It is measured by the method explained at section 3. The code would measure the peaks and trough points, then extract the identified displacement curve automatically.

6. CONCLUSION

An easy method with an error shown to be less than 7% of estimating the spool displacement of a high-speed on/off solenoid valve is presented. This method can estimate the valve spool displacement depending on a sensorless strategy, where no displacement sensor is used. If a displacement sensor is used, modification to valve construction is required, so the valve damage probability increases or the system may suffer from contamination problems.

The proposed method helps the researchers and users not only to estimate the spool displacement but also to accurately identify the dynamic behavior of the valve. Which can make modeling and controlling the solenoid valve be more easy and simple than the traditional methods.

REFERENCES

[1] Bolton, W. (2019). Mechatronics: Electronic control systems in mechanical and electrical engineering. Pearson Education.

[2] Dong, S., et al. (2019). "High-efficiency aircraft antiskid brake control algorithm via runway condition identification based on an on-off valve array." Chinese Journal of Aeronautics **32**(11): 2538-2556.

[3] Gabitov, I., et al. (2021). "Development of a Method for Diagnosing Injectors of Diesel Engines." Communications-Scientific letters of the University of Zilina 23(1): B46-B57.

[4] Тан, H., G. Hy (2016). "HSV reverse design and optimization of impact system and pneumatic system of the rotary hammer." Machine Tool & Hydraulics **2016**: 17.

[5] Wang, S., et al. (2020). "A Performance Improvement Strategy for Solenoid Electromagnetic Actuator in Servo Proportional Valve." Applied Sciences **10**(12): 4352.

[6] Chen, X., et al. (2021). "Characteristic investigation of a magnetostrictive fast switching valve for digital hydraulic converter." Proceedings of the Institution of Mechanical Engineers, Part I: Journal of Systems and Control Engineering **235**(2): 190-206.

[7] Gao, Q., et al. (2020). "Investigation on adaptive pulse width modulation control for high speed on/off valve." Journal of Mechanical Science & Technology **34**(4).

[8] Gandomzadeh, D. and M. H. Abbaspour-Fard (2020). "Numerical study of the effect of core geometry on the performance of a magnetostrictive transducer." Journal of Magnetism and Magnetic Materials **513**: 166823.

[9] Mohith, S., et al. (2020). "Recent trends in piezoelectric actuators for precision motion and their applications: A review." Smart Materials and Structures.

[10] Meng, F., et al. (2021). Time Delay Characteristics Analysis of Pressure Dynamic Response on Electro-hydraulic Pressure Regulating valve. 2021 4th IEEE International Conference on Industrial Cyber-Physical Systems (ICPS), IEEE.

[11] Jing-jun, L., et al. (2021). "Dynamic Switching Response of Solenoid Valve Based on Maxwell." CHINESE HYDRAULICS & PNEUMATICS **45**(4): 123.

[12] Damljanović, D. and B. Rašuo (2010). "Testing of calibration models in order to certify the overall reliability of the trisonic blowdown wind tunnel of VTI." FME Transactions **38**(4): 167-172.

[13] Kang, J.-Y. and Y.-H. Jeon (2018). "Position Control for Solenoid Valve using the Fractional Order Controller." The Journal of the Korea institute of electronic communication sciences **13**(1): 101-106.

[14] Malaguti, F. and E. Pregnolato (2002). Proportional control of on/off solenoid operated hydraulic valve by nonlinear robust controller. Industrial Electronics, 2002. ISIE 2002. Proceedings of the 2002 IEEE International Symposium on, IEEE.

[15] Lunge, S. P., et al. (2013). Proportional actuator from on off solenoid valve using sliding modes. Proceedings of the 1st International and 16th National Conference on Machines and Mechanisms (iNaCoMM2013).

[16] Dinulović, M., et al. (2020). "Numerical modeling of Nomex honeycomb core composite plates at meso scale level." FME Transactions **48**(4): 874-881.

[17] Hammond, P. W. (2012). Position sensor for mechanically latching solenoid, Google Patents.

[18] Lee, J.-H., et al. (2015). "Control of spool position of on/off solenoid operated hydraulic valve by sliding-mode controller." Journal of Mechanical Science and Technology **29**(12): 5395-5408.

[19] Scheidl, R., et al. (2014). Investigation of a switch-off time variation problem of a fast switching valve. ASME/BATH 2014 Symposium on Fluid Power and Motion Control, American Society of Mechanical Engineers Digital Collection.

[20] Zhong, Q., et al. (2017). "Performance analysis of a high-speed on/off valve based on an intelligent pulse-width modulation control." Advances in Mechanical Engineering **9**(11): 1687814017733247.

[21] Braun, T., et al. (2018). "Observer design for self-sensing of solenoid actuators with application to soft landing." IEEE Transactions on Control Systems Technology **27**(4): 1720-1727.

[22] Yudell, A. C. and J. D. Van de Ven (2015). "Predicting solenoid valve spool displacement through current analysis." International journal of fluid power **16**(3): 133-140.

[23] Cetinkunt, S. (2015). Mechatronics with experiments, John Wiley & Sons.

[24] BillingsleyUniversity, J. (2009). "Mechatronic Systems, Sensors, and Actuators: Fundamentals and Modeling."

[25] Badr, M. (2018). Modelling and Simulation of a Controlled Solenoid. IOP Conference Series: Materials Science and Engineering, IOP Publishing.

[26] Lyshevski, S. E. (2017). Mechatronics and Cont–rol of Electromechanical Systems, CRC Press.

[27] Jin, L. and Q. Wang (2018). "Positioning control of hydraulic cylinder with unknown friction using on/off directional control valve." Proceedings of the Institution of Mechanical Engineers, Part I: Journal of Systems and Control Engineering **232**(8): 983-993.

[28] Szpica, D. and M. Kusznier (2021). "Model evaluation of the influence of the plunger stroke on functional parameters of the low-pressure pulse gas solenoid injector." Sensors 21(1): 234.

[29] Rabie, M. G. (2009). Fluid power engineering/M. Galal Rabie, New York: McGraw-Hill.

[30] Malm, R. (2015), Instrumentation and evaluation of the concrete dome plug domplu, Technical report, KTH Royal Institute of Technology.

[31] Ćalasan, M., et al. (2020). "On the root mean square error (RMSE) calculation for parameter estimation of photovoltaic models: A novel exact analytical solution based on Lambert W function." Energy conversion and management **210**: 112716.

ПРОЦЕНА ПОЛОЖАЈА БЕЗ СЕНЗОРА И ИДЕНТИФИКАЦИЈА ВРЕМЕНА ПРЕЛАЗА ЗА КАЛЕМ ЕЛЕКТРОМАГНЕТНОГ ВЕНТИЛА ВЕЛИКЕ БРЗИНЕ ЗА УКЉУЧИВАЊЕ/ ИСКЉУЧИВАЊЕ

А.Н. Аброба, К.А. Гамри, А. Салех, М.Х. Мабрук

У овом раду је приказана метода за детекцију положаја калема брзог укљ./искљ. соленоидног

вентила без сензора. Метода зависи од анализе временско-струјне криве проласка струје соленоида и мерења максималног хода калема вентила, тако да се процењује динамичко понашање вентила и приказује крива померања калема. Развијен је математички модел електромагнетног вентила и проучаван је утицај хидрауличке силе на калем вентила. Експериментални резултати показују да је грешка предложене методе мања од 7% у поређењу са помаком калема вентила који се мери уобичајеним линеарним претварачем променљивог помака.